HHS Public Access

Author manuscript

J Immunol. Author manuscript; available in PMC 2017 August 15.

Published in final edited form as:

J Immunol. 2016 August 15; 197(4): 1389–1398. doi:10.4049/jimmunol.1502432.

NETRIN-1 AUGMENTS CHEMOKINESIS IN CD4+ T CELLS *IN VITRO* AND ELICITS A PROINFLAMMATORY RESPONSE *IN VIVO*[1]

Leo Boneschansker[*,†], **Hironao Nakayama**[‡], **Michele Eisenga**[*], **Johannes Wedel**[*], **Michael Klagsbrun**[‡], **Daniel Irimia**[†], and **David M Briscoe**[*,2]

[*]Transplant Research Program and The Division of Nephrology, Department of Medicine, Boston Children's Hospital, Boston, MA, and the Department of Pediatrics, Harvard Medical School, Boston, MA

[†]Center for Engineering in Medicine, Department of Surgery, Massachusetts General Hospital, Harvard Medical School, Shriners Hospitals for Children, Boston, MA

[‡]Vascular Biology Program, Department of Surgery, Boston Children's Hospital, Harvard Medical School, Boston, MA

Abstract

Netrin-1 is a neuronal guidance cue that regulates cellular activation, migration and cytoskeleton rearrangement in multiple cell types. It is a chemotropic protein that is expressed in multiple tissues and elicits both attractive and repulsive migratory responses. Netrin-1 has recently been found to modulate the immune response via the inhibition of neutrophil and macrophage migration. However, the ability of Netrin-1 to interact with lymphocytes, and its in-depth effects on leukocyte migration is poorly understood. Here, we profiled the mRNA and protein expression of known Netrin-1 receptors on human $CD4^+$ T-cells. Neogenin, UNC5A and UNC5B were expressed at low levels in unstimulated cells, but increased following mitogen-dependent activation. By immunofluorescence, we observed a cytoplasmic staining pattern of neogenin and UNC5A-B that also increased following activation. Using a novel microfluidic assay, we found that Netrin-1 stimulated bi-directional migration and enhanced the size of migratory subpopulations of mitogen-activated $CD4^+$ T-cells, but it had no demonstrable effects on the migration of purified $CD4^+CD25^+CD127^{dim}$ T regulatory cells. Furthermore, using a shRNA knockdown approach, we observed that the pro-migratory effects of Netrin-1 on T effectors is dependent on its interactions with neogenin. In the humanized SCID mouse, local injection of Netrin-1 into skin enhanced inflammation and the number of neogenin-expressing $CD3^+$ T cell infiltrates. Neogenin was also observed on $CD3^+$ T cell infiltrates within human cardiac allograft biopsies with evidence of rejection. Collectively, our findings demonstrate that Netrin-1/neogenin

[1]Research reported in this publication was supported in part by National Institutes of Health grants R01AI092305 and AI04675 (to DMB), and by GM092804 (to DI) and in part by the Casey Lee Ball Foundation (to DMB). LB was supported by NIH grants T32DK07726 and T32AI007529. All microfabrication was performed at the NIBIB funded, BioMEMS Resource Center (EB002503).

[2]Address for Correspondence: David M. Briscoe, Transplant Research Program, Division of Nephrology, Boston Children's Hospital, 300 Longwood Ave, Boston, MA 02115; david.briscoe@childrens.harvard.edu.

interactions augment $CD4^+$ T cell chemokinesis and promote cellular infiltration in association with acute inflammation in vivo.

Introduction

Axonal guidance molecules belong to at least four families, namely Netrins, Semaphorins, Slits, and Ephrins, and they regulate cellular activation, migration and cytoskeleton rearrangement in multiple cell types (1–3). An increasing number of reports indicate that guidance receptors are also expressed on leukocyte subsets where they primarily function to regulate migration (4–7). For instance, the binding of class 3 semaphorin family molecules to the neuropilin-1 receptor results in anti-migration and cytoskeletal collapse in multiple cell types including leukocytes (8–10). Slit-Robo interactions inhibit chemokine-induced leukocyte migration, and protect against neutrophil-induced ischemia-reperfusion injury (6, 11, 12). In addition, Ephrins are reported to function in chronic inflammation by enhancing both T-cell maturation and leukocyte trafficking, for instance in rheumatoid arthritis (13, 14).

The Netrins, and specifically Netrin-1 is a more recently described guidance cue with unique effects on the immune response (4, 15, 16). It is a major growth and pro-migratory chemotactic factor (17), and it has been reported to elicit chemoinhibitory responses in bulk populations of leukocytes (4, 15, 18). Netrin-1 is a secreted laminin-related protein that mediates signalling through seven receptors, namely members of the Uncoordinated-5 family (UNC5A–D), Deleted in Colorectal Cancer family (DCC), Neogenin, and Down Syndrome Cell Adhesion Molecule (DSCAM) (19). The binding of Netrin-1 to the UNC5 family of receptors promotes axonal chemorepulsion, whereas its binding to neogenin and/or DCC promotes chemoattraction (19). Initial reports demonstrated that the UNC5 family of receptors were expressed at high levels by human peripheral blood leukocytes and that Netrin-1 inhibits migration towards chemotactic stimuli *in vitro* in transwell assays (4). Furthermore, several additional reports indicate that it elicits potent anti-inflammatory effects in models of peritonitis (4, 18), acute lung injury (20), hypoxia-induced inflammation (21), acute colitis (22) as well as in kidney ischemia/reperfusion injury (15). In these and other studies, Netrin-1 was proposed to dominantly function via interactions with UNC5-family receptors (4, 15, 16, 20–22).

However, more recent studies suggest that the effects of Netrin-1 may be more complex (19, 23). For example, in an atherosclerosis model, Netrin-1 was found to retain macrophages within plaques by inhibiting macrophage emigration from the inflammatory site (5); also Netrin-1 has been found to promote chronic inflammation in adipose tissue (24). Several studies have evaluated Netrin-1 receptor biology using neogenin knockout mice which mount a reduced inflammatory peritonitis reaction (25), have less leukocyte infiltrates and reduced inflammation in models of acute lung injury (26) and ischemia reperfusion injury (27).

These collective studies allow for the possibility that both chemoattractive/neogenin and chemorepulsive/UNC5-family receptors may be co-expressed on subsets of leukocytes and that the relative expression of the pro-migratory receptor neogenin may determine the ability of Netrin-1 to elicit a pro- vs. an anti-inflammatory response. However, little is known about

Netrin-1/Netrin receptor interactions in $CD4^+$ T cells and adaptive immunity. In these studies, we used a novel *in vitro* microfluidic assay to evaluate the effects of Netrin-1 on migration of $CD4^+$ T cells at the single cell level. Our findings demonstrate that Netrin-1 induces bi-directional migratory responses, and that it increases the size of migratory subpopulations of mitogen-activated $CD4^+$ T-cells. Furthermore, we observed that Netrin-1 primarily regulates T effector migration and does not alter the migration of purified populations of $CD4^+CD25^+CD127^{dim}$ T regulatory cells. In addition, we find that these biological effects of Netrin-1 on CD4+ T cell migration are dependent on the expression of neogenin. Finally, we evaluated its function *in vivo* and found that the administration of Netrin-1 into human skin in the huSCID mouse augmented the recruitment of $CD3^+$ T cells within the local inflammatory response. In addition we observed high levels of neogenin expression on T cell infiltrates within the inflamed skin. Neogenin was also expressed on $CD3^+$ T cell infiltrates within endomycardial biopsies from human cardiac transplant recipients, further suggesting that it is of great pathophysiological significance. Together, our findings for the first time indicate that the primary function of Netrin-1 is to augment chemokinesis of activated $CD4^+$ T effector cells. Furthermore, we show that this function of Netrin-1 is elicited via interactions with neogenin. Our findings are most suggestive that Netrin-1/neogenin interactions function to augment T cell recruitment into sites of acute inflammation including allografts undergoing rejection.

Materials and Methods

Reagents

Anti-human UNC5A and -Neogenin antibodies were purchased from Santa Cruz Biotechnology (Dallas, TX), anti-UNC5B or -DCC from Abcam (Cambridge, MA) and anti-CD3 antibody from Dako (Carpinteria, CA). Goat anti-mouse Alexa fluor 488 and goat anti-rabbit Alexa fluor 594 were purchased from Life Technologies (Carlsbad, CA). Human Netrin-1 was produced as previously described (23). Briefly, 293T cells were transfected with netrin-1/pcDNA3.1/V5-His-TOPO plasmid using FuGENE HD Transfection Reagent (Roche Applied Science, Indianapolis, IN) and secreted Netrin-1 was purified from the culture medium using HiTrap HP Chelating columns (GE Healthcare Bio-Sciences, Pittsburgh, PA), as described (28). Anti-human CD3 and anti-human CD28 were purchased from BD Pharmingen (San Jose, CA) and Phytohaemagglutinin (PHA) from Fisher Scientific (Pittsburgh, PA).

$CD4^+$ T-lymphocyte culture

Human blood samples were obtained from healthy volunteers consented in accordance with IRB approval by Boston Children's Hospital. PBMC were harvested by gradient centrifugation (2200 rpm for 30 minutes) using Ficoll (GE Healthcare, Waukesha, WI) and $CD4^+$ T cells were positively isolated from the PBMC using magnetic beads (Dynabeads $CD4^+$ isolation kit, Invitrogen, Carlsbad, CA) according to the manufacturer's protocol. $CD4^+CD25^+$ and $CD4^+$ $CD25^{neg}$ T-lymphocytes were isolated by positive selection, and the $CD127^{dim}$ subset of $CD4^+$ $CD25^+$ T regulatory cells were isolated by a subsequent negative selection using the Human $CD4^+CD127loCD25^+$ Regulatory T Cell Isolation Kit (Stemcell technologies, Vancouver, Canada) according to the manufacturer's protocol. $CD4^+$ T-

lymphocyte subsets were cultured in RPMI 1640 media (Cambrex, Charles City, IA) containing 10% fetal bovine serum, 2 mM L-glutamine, 100 U mL-1 penicillin/streptomycin (Gibco-Invitrogen), 1% sodium bicarbonate and 1% sodium pyruvate (Cambrex). $CD4^+$ T-cells were used immediately or following a freeze thaw (occasionally) and were activated with anti-human CD3 and anti-human CD28 (each at 1 μg/mL) or Phytohaemagglutinin (PHA, 2.5 μg/mL) for intervals of 6–48hrs. $CD4^+CD25^{neg}$ T cells were cultured in medium (above), stimulated with 1 μg/ml plate-bound anti-CD3 antibody in the absence or presence of different concentrations of netrin-1 (0.1–1 μg/ml).

Real-time PCR

Total RNA was isolated from $CD4^+$ T-cells following mitogen activation using the RNeasy isolation kit (Qiagen, Valencia, CA). cDNA was generated using qScript Supermix (Quanta Biosciences, Gaitherburg, MD), according to the manufacturer's instructions. The qRT-PCR primers used in the present study are as follows: UNC5A, forward 5′-TCTACCTCACGCTGCACAAG-3′ and reverse 5′-AGTGGTCCATAGCCAGGATG-3′; UNC5B, forward 5′-TCCAGCTGCATACCACTCTG-3′ and reverse 5′-GGATGGACAGTGGGATCTTG-3′; UNC5C, forward 5′-AGCAAGGCAGACTGATCCAT-3′ and reverse 5′-TCAGCAAGCTGACTCCTGAA-3′; UNC5D, forward 5′-AGTGGGTCCATCAGAACGAG-3′ and reverse 5′-CATGGAAGTCCTCCACCTGT-3′; Neogenin, forward 5′-GTGTTGCCATGTGTTGCTTC-3′ and reverse 5′-ACCTGCCAGCAATACCAATC-3′; DCC, forward 5′-AGGTCGTCATGGAGATGGAG-3′ and reverse 5′-TCACAAGCAGGTTGCTGTTC-3′; DSCAM, forward 5′-CGAATGCACATCGACATACC-3′ and reverse 5′-TCAGCATCCGTCAACAGAAC-3′; GAPDH, forward 5′-ACCACAGTCCATGCCATCAC-3′ and reverse 5′-TCCACCACCCTGTTGCTGTA-3′; IFN-γ, forward 5′-TCGGTAACTGACTTGAATGTCCA-3′ and reverse 5′-TCGCTTCCCTGTTTTAGCTGC-3′; IL-2, forward 5′-AACTCCTGTCTTGCATTGCAC-3′ and reverse 5′-GCTCCAGTTGTAGCTGTGTTT-3′; IL-4, forward 5′-CCAACTGCTTCCCCCTCTG-3′ and reverse 5′-TCTGTTACGGTCAACTCGGTG-3′; IL-5, forward 5′-TCTACTCATCGAACTCTGCTGA-3′ and reverse 5′-CCCTTGCACAGTTTGACTCTC-3′; IL-6, forward 5′-ACTCACCTCTTCAGAACGAATTG-3′ and reverse 5′-CCATCTTTGGAAGGTTCAGGTTG-3′; IL-10, forward 5′-TCAAGGCGCATGTGAACTCC-3′ and reverse 5′-GATGTCAAACTCACTCATGGCT-3′; IL-17A, forward 5′-AGATTACTACAACCGATCCACCT-3′ and reverse 5′-GGGGACAGAGTTCATGTGGTA-3′; B2M, forward 5′-TTTCATCCATCCGACATTGA-3′ and reverse 5′-CCTCCATGATGCTGCTTACA-3′. Primers and cDNA where mixed with SYBR Green Supermix (Quanta Biosciences, Gaitherburg, MD) and real-time PCR was performed using the 7300 real-time PCR system (Applied Biosystems, Foster City, CA). A comparative threshold cycle (CT) value was normalized for each sample using the formula: ΔCT = CT (gene of interest) − CT (GAPDH or B2M). The relative expression was then calculated according to the $2^{-\Delta CT}$ method.

Western Blot Analysis

Cells were lysed with radioimmunoprecipitation assay buffer (Boston Bioproducts, Boston, MA) and protease and phosphatase inhibitors (Thermo Scientific, Rockford, IL) were added. Proteins were separated on a Mini-protean TGX precast gel (Bio-Rad Laboratories, Hercules, CA) and transferred onto a polyvinylidene difluoride membrane (Millipore, Billerica, MA). Membranes were blocked with 4% skimmed milk in Tris-buffered saline and 0.1% Tween-20 for 1 hour and incubated with primary antibodies (as indicated) overnight at 4°C. Membranes were subsequently washed and incubated with a species-specific secondary peroxidase-linked antibody for 90 minutes at room temperature, and the protein of interest was detected by chemiluminescence (Thermo Scientific, Tewksbury, MA).

Flow Cytometry

$CD4^+$ T-lymphocytes were stained with unconjugated anti-Neogenin or a rabbit IgG isotype antibody (GeneTex, Irvine, CA) as a control for 30 min at 4°C. Cells were subsequently washed and incubated with species-specific secondary FITC-conjugated antibody for 30 min at 4°C. Data was acquired on a FACsCalibur (BD Biosciences) and analyzed using FlowJo software (Tree Star, Ashland, OR).

Cellular Immunofluorescence

Unactivated and 48h mitogen-activated (PHA 2.5 μg/mL) cells were plated onto ImmunoSelect adhesion slides (MoBiTec, Duesseldorf, Germany), washed and blocked with 5% bovine serum albumin (Fisher Scientific, Pittsburgh, PA) in PBS. The cells were subsequently incubated with primary antibodies or a rabbit IgG isotype control antibody for 60 min at room temperature. After washing in PBS, cells were incubated with secondary antibody for 1 hour. Finally, cells were mounted with Prolong Gold antifade with DAPI (Life Technologies) and staining was evaluated by microscopy using a Nikon Eclipse 80i microscope and a Retiga-2000R CCD Camera (QImaging, Surrey, Canada). Each image was collected and processed using NIS Elements (Version 3.2) software. Images were analyzed using Image J (NIH).

Short hairpin RNA knockdown

Lentivirus was produced with 293T cells, using the pPACKH1 HIV Lentivector packaging kit and Purefection (System Biosciences, Mountain View, CA), together with neogenin shRNA plasmids (NEO1 Mission shRNA plasmids: shNeo-1:TRCN0000311710 and shNeo-2:TRCN0000118046) or a control shRNA (Mission pLKO.1-puro non-target shRNA, Sigma-Aldrich, St. Louis, MO), according to the manufacturer's protocol. In all experiments, $CD4^+$ T-cells were activated for 48h (with anti-CD3/CD28) and simultaneously transfected with lentivirus containing Neo-shRNA or control shRNA. Cells were infected with shControl or ShNEO1 lentivirus using a range of MOI from 10–15.

Migration experiments

Migration of $CD4^+$ T-cell subsets was analyzed in microfluidic devices designed for the analysis of bi-directional migration patterns live-time, as described previously (12). Briefly, three layers (3, 10 and 50 μm thick) of negative photoresist (SU8, Microchem, Newton, MA)

were patterned on a silicon wafer by sequentially employing three photolithography masks and processing cycles, according to the manufacturer's instructions. The wafer with patterned photoresist was used as a mold to produce PDMS (Polydimethylsiloxane, Fisher Scientific, Fair Lawn, NJ) parts, which were subsequently bonded irreversibly to standard glass slides (75×25 mm, Fisher Scientific). The microfluidic devices were primed with chemoregulatory protein(s) 30 minutes prior to loading of the device with T cells. Netrin-1 and/or RANTES/CCL5 (Biolegend, San Diego, CA) were instilled into the device (~20μL) in combination with 100 nM human fibronectin (Sigma-Aldrich) in cell culture media. After 15 minutes the solution was washed out of the device using complete media. Passive diffusion of chemoregulatory protein(s) from the reservoirs into the main channel creates a gradient from the reservoir (highest concentration) to the buffer channel (lowest concentration). Subsequently, 2×10^5 cells are gently delivered into the cell-loading chamber, where the cells are evenly distributed in the cell loading traps, from where they can migrate into 10 μm wide migration channels. Cell migration is recorded using time-lapse imaging on a fully automated Nikon TiE microscope (10× magnification) with biochamber heated to 37 °C with 5% carbon dioxide gas, for 8 hours. Cell displacement was tracked manually using Image J (NIH).

Analysis of cell migration

Cell migration inside migration channels was analyzed, as previously described (12), using four parameters: 1) the percentage of migrating cells; 2) the direction of migration; 3) the speed of migration; and 4) the directional persistence (DP) following migration. The *percentage of migrating cells* was evaluated as the number of cells migrating in each direction as a ratio of the total number of cells loaded in the cell reservoir. The *direction of migration* was evaluated as a response either towards or away from the chemokine. *Speed* was calculated by the total distance traveled divided by the duration of migration, and *DP* was determined by comparing the relative displacement of cells from their initial to their final position within the migration channel as a ratio of the total distance traveled over the 8-hr period of migration. Cells migrating persistently towards the chemokine reservoir without changing direction were determined to have a DP equal to "1", and cells migrating persistently away from the gradient have a DP equal to "−1". DP values smaller than 1 identify cells that change direction in the course of migration. For instance, a DP value equal to "0" reflects cells that migrate back and forth through the migration channels and ultimately return to their initial starting position by the end of the experiment.

Humanized SCID mouse model

Human neonatal foreskins were obtained from the birthing unit at the Brigham and Women's Hospital in accordance with IRB approval. The skin was prepared under sterile conditions and was transplanted onto severe combined immunodeficient (SCID) mice. Once healed after approximately 6 weeks, the mice were humanized by intraperitoneal injection of 3×10^8 human PBMCs. At days 0 and 7 following humanization, growth factor reduced matrigel (BD Biosciences, Bedford, MA) combined with Netrin-1 (5μg diluted in sterile PBS) was injected intradermally into the skin graft. Injection of matrigel with PBS served as a control. After 14 days, the mice were euthanized and the skin grafts were harvested for evaluation by histology. Each skin was divided into two parts, one of which was frozen in

liquid N2/O.C.T. compound (Sakura Finetek, Torrance, CA) for later cryosectioning and histochemistry; the other part was fixed in formalin and embedded in paraffin, for processing with H&E staining.

Immunohistochemistry/Immunofluorescence

Skin grafts were cut into four-micron cryosections and were initially blocked with 0.3% hydrogen peroxide or 10% serum (host of secondary antibody) in 0.05% Tris-tween, washed and incubated with the primary antibody for 1 hour. Control sections were incubated with a species-specific IgG. After washing in PBS, sections were incubated with a secondary species-specific HRP-conjugated or fluorescent-tagged antibody for 1 hour. For immunohistochemistry, staining was resolved using amino-ethyl carbazole and the slides were mounted in glycerol gelatin (Sigma-Aldrich, St. Louis, MO); for immunofluorescence, the sections were mounted with VectorShield mounting medium with DAPI (Vector Laboratories, Burlingame, CA).

Human endomyocardial biopsies were collected from cardiac transplant recipients during routine post-transplantation care and were stored at −80°C until use in this study. Collection was approved by the Human Research Committee, Brigham and Women's Hospital, Boston, MA. Research studies were performed after clinicopathologic diagnoses and clinical care was completed. Four-micron cryosections were prepared as described above and stained with anti-human CD3 and anti-human Neogenin, as above. Staining of skin and heart was evaluated by microscopy using a Nikon Eclipse 80i microscope and a Retiga-2000R CCD Camera (QImaging, Surrey, Canada). Confocal microscopy imaging was performed using an Olympus FV1000 microscope (Olympus Scientific Solutions, Waltham, MA).

Statistical analysis

Statistical significance was determined using the student t test or 1 way ANOVA for normally distributed data and the Mann Whitney test for data that did not have normal distribution. Differences were considered statistically significant when p values were less than 0.05.

Results

Neogenin is the dominant Netrin-1 receptor expressed by activated CD4$^+$ T-lymphocytes

Purified human CD4$^+$ T-cells were initially profiled at the mRNA level for known Netrin-1 receptors. Using quantitative PCR, we found neogenin, UNC5A and UNC5B and low levels of DCC on unactivated cells (Fig 1A–C and Fig S1A); in contrast, UNC5C-D and DSCAM were not expressed at any significant level (data not shown). Following mitogenic-activation with anti-CD3/anti-CD28, there was a marked time-dependent increase in the expression of neogenin over 6 to 48 hrs (average 7-fold, Fig 1A), and a smaller increase in UNC5B expression (~1.5 fold, Fig 1C). No change in UNC5A mRNA expression was observed (Fig 1B; Ct value >30). By Western blot analysis (Figs 1D–E), neogenin, UNC5A and UNC5B were expressed by unactivated CD4$^+$ T cells and expression of neogenin notably increased (~3.5 fold) following activation with PHA (Fig 1D–E) or anti-CD3/CD28 (not shown). Induced expression of neogenin was also evident by flow cytometry (Fig 1F) following

48hrs mitogenic activation of $CD4^+$ T cells. UNC5A increased in expression following mitogenic activation, but to a lesser degree than neogenin (~1.5 fold; Fig 1D, E), and UNC5B expression was also induced (~2.5 fold) following activation. We failed to observe expression of DCC at the protein level (Fig S1B). Immunofluorescent staining of unactivated $CD4^+$ T-cells showed minimal neogenin and UNC5A, and detectable levels of UNC5B expression. However, staining of neogenin and UNC5B was prominent following 48hrs activation with PHA (2.5μg/mL, Fig 2). Thus, both chemoattractive (neogenin) and chemorepulsive (UNC5A and UNC5B) Netrin-1 receptors are expressed by $CD4^+$ T cells, and each receptor is modulated following cellular activation.

Netrin-1 increases the size of migratory subpopulations of activated $CD4^+$ T cells

To next determine the effects of Netrin-1 on $CD4^+$ T cell migration, we used a microfluidic device that allows for the quantitative analysis of bi-directional trafficking at single cell resolution ((12) and Fig 3A). Initially, positively selected $CD4^+$ T cells were mitogen-activated (48hrs) and introduced into the device, and exposed to increasing concentration gradients of Netrin-1 over an 8-hr time period (Fig 3B). Their migration characteristics were compared to cells in culture media alone as a control. We found that all concentrations of Netrin-1 enhance the number of migrating T-cells from 19.0±5.1% (media control) to 41.9±12.2%, 37.5±15.7%, and 28.1±12.6% in Netrin-1 concentrations of 0.1μg/mL, 0.5μg/mL or 5μg/mL respectively (Fig 3B, $p<0.05$; Supplementary Movie 1 and 2). Netrin-1 increased the number of cells migrating towards the gradient from 8.8±2.9% (in media alone) to 21.5±5.1% (in 0.1μg/mL). It also increased the number of cells migrating away from the gradient from 10.2±2.6% (in media alone) to 18.2±7.3% (in 0.1μg/mL Netrin-1, Fig 3B; $p<0.05$). Increasing the concentration of Netrin-1 did not change these bi-directional migration patterns.

We next examined the effect of Netrin-1 on the migration of $CD4^+$ subpopulations including $CD4^+CD25^{neg}$ naïve and $CD4^+CD25^+CD127^{dim}$ T regulatory subsets. Similar to pooled populations of $CD4^+$ cells (12), we found that low numbers of $CD4^+CD25^{neg}$ cells migrate within the device in media alone (12.3±3.5%) but this subset demonstrated an induced migratory response to a Netrin-1 gradient (17.8±3.0% in 0.1μg/mL Netrin-1, Fig S2A). However, surprisingly few T regs were observed to migrate within the device in media alone (7.6±4.6% cells migrating), and the addition of Netrin-1 failed to increase or decrease the numbers of migrating cells (6.4±3.6%) or their directional migratory pattern over an 8hr period (Fig. S2A–B). In general, we observed that T regs migrate in low numbers within the device and fail to respond to Netrin-1 even following mitogen-dependent activation (data not shown). Consistent with these functional observations, T reg subsets express minimal cell surface neogenin (data not shown). Collectively, these findings are suggestive that Netrin-1 stimulates bi-directional migratory responses in activated $CD4^+$ T effector cells by increasing the size of migratory subpopulations.

$CD4^+$ T effector-cell migration is induced by Netrin-1

We next wished to map the individual migratory trajectory of Netrin-1-responsive $CD4^+$ T cells and calculate an overall Directional Persistence (DP), as previously described (12). Using the DP algorithm, we find that Netrin-1 favors persistent migration of $CD4^+$ T cells

towards the gradient (DP=0.18 vs. DP=0.06 in media alone, $p<0.05$, Fig 3C). We also analyzed the initial migration response for every cell during the 8-hour observation period. We find that the fraction of the total cell population that migrates within the first hour increases from ~1.5% (in media alone) to ~7% in the presence of Netrin-1 ($p<0.05$). As shown in Fig 4A, the effect of Netrin-1 on the induction of migration was prominent in the first 3 hours. The average speed of cells migrating in the direction of the Netrin-1 gradient did not increase (10.3 ± 4.2 μm/min) as compared to culture medium alone (9.9 ± 4.7 μm/min, Fig. 4C). The speed of migration away from the Netrin-1 gradient was also comparable to the response in media (Fig. 4B). Collectively, these findings indicate that the total fraction of migrating $CD4^+$ cells increases in the presence of Netrin-1, and that Netrin-1 favors persistent migration towards a gradient without affecting speed.

Minimal effect of Netrin-1 on RANTES-induced migration

Since our studies indicate that Netrin-1 functions to increase the size of migratory subpopulations, we next wished to determine if it alters migration towards established chemokines. We used RANTES (100nM) as a reference chemoattractant chemokine, as we described previously using another microfluidic device (29). As expected, we found that RANTES induced a marked chemoattractant response in 22.2±5.0% of mitogen-activated $CD4^+$ T cells in our microfluidic device. However, when Netrin-1 (0.1μg/mL) was combined with RANTES, the chemoattractant response did not change significantly (chemoattraction in 22.2±9.5% cells, Fig 5A). RANTES also increased migration speed vs. cells in media alone (12.1 ± 5.2 μm/min vs. 10.9 ± 5.2 μm/min; $p<0.01$), and the combination of Netrin-1 with RANTES failed to change this response significantly (Fig 5B). Thus, Netrin-1 does not enhance or inhibit the pro-migratory effects of the chemoattractant chemokine RANTES.

Netrin-1-Neogenin interactions function to augment migration of $CD4^+$ T cells

Due to its high level of expression, we postulated that neogenin interactions regulate responsiveness in activated $CD4^+$ cells. To test this possibility, we infected human $CD4^+$ T-cells with two different neogenin shRNA lentiviral constructs (knockdown efficiency of 50–70%, Fig S3) or a control shRNA, and we evaluated migration in response to Netrin-1. As illustrated in Fig. 6A, we found that the bi-directional migratory response to Netrin-1 was significantly reduced in neogenin shRNA-infected cells as compared to control shRNA infected cells ($p<0.05$). There was a prominent inhibitory effect on the migratory response towards Netrin-1 (11.3±4.1% in controls vs. 2.9±1.8% in shRNA infected cells, $p<0.05$, Fig 6B) as well as on the migratory response away from Netrin-1 (10.3±3.4% in controls and 4.3±3.7% in shRNA infected cells, $p<0.05$, Fig 6B). These findings are most suggestive that neogenin functions as a pro-migratory/chemokinetic receptor and does not confer preferential directionality to cells within the Netrin-1 gradient. Furthermore, they suggest that the Netrin-1-induced migratory response is a function of random neogenin-regulated chemokinesis.

Effects of Netrin-1 on T cell activation

Previous work has shown that Netrin-1 binds the UNC family of receptors on murine $CD4^+$ T-cells to inhibit cytokine production (15). Although, we observed minimal expression of UNC5A/B on human $CD4^+$ T cell subsets, we also wished to determine if Netrin-1 regulates

activation responses. Freshly isolated $CD4^+CD25^-$ T cells were cultured with plate bound anti-CD3 (1μg/mL) for 24–48hrs in the absence or presence of increasing concentrations of Netrin-1 (0.1–1μg/mL). Cytokine production (IL-2, IL-4, IL-5, IL-6, IL-10, IL-17A and IFN-γ) was evaluated at the mRNA level. We observed a marked increase in cytokine production in anti-CD3 treated cells, and co-culture with Netrin-1 failed to alter this activation response (Fig. S4, and data not shown). In addition, coculture of iTregs with Netrin-1 failed to alter the expansion of $CD4^+CD25^{hi}FoxP3^+$ T cells in vitro (data not show). Thus, Netrin-1 does not regulate mitogen-dependent activation in human CD4+ T cell subsets, consistent with their low levels of expression of UNC5-family molecules.

Pathophysiological significance of Netrin-1/Neogenin interactions in vivo

Next, we wished to evaluate the effect of Netrin-1 on the recruitment of T cells into sites of inflammation *in vivo*. For these studies, we initially used a humanized SCID mouse model that is well established in our laboratory (30–33). In this model, human skin is allowed to engraft onto SCID mice over a 6-week period, after which 3×10^8 human PBMCs are adoptively transferred by i.p injection. Netrin-1 (5μg in matrigel) was injected intradermally into the transplanted human skin on day 0 and day 7 post-transfer, and the skin was harvested on day 14 for evaluation of leukocytic infiltrates (Fig 7A); intradermal injection of matrigel/PBS alone served as a negative control. By H&E staining, we observed focal leukocytic infiltrates within control skins harvested from humanized mice (307±58 cells/hpf, Fig 7B). In contrast, diffuse infiltrates were present throughout skins following intradermal injection of Netrin-1 (466±24 cells/hpf, Fig 7B). Overall, by semi-quantitative grid counting there was an approximate 1.5 fold increase ($p<0.01$) in infiltrates in Netrin-1 injected skins, as compared to negative control skins (Fig 7B). By immunohistochemistry using anti-CD3, there was an approximate twofold increase in the number of T cell infiltrates in Netrin-1 injected skins vs. negative controls (162±59 T-lymphocytes/hpf vs. 86±51, $p<0.01$, Fig 7C).

We also analyzed the expression of neogenin on $CD3^+$ T cells within the harvested skin tissue. Interestingly, we found diffuse expression of neogenin throughout the skin grafts (Fig 7D) on infiltrates as well as on interstitial cells and blood vessels. Using double immunofluorescence staining, we found marked co-localization of the neogenin receptor on $CD3^+$ T cells (Fig 7E), suggesting that infiltrating neogenin-expressing T cells respond to Netrin-1 in vivo.

Finally, we analyzed the colocalzation of neogenin with $CD3^+$ infiltrates in human endomyocardial allograft biopsies (n=6) with varying degrees of rejection. By grid counting, we found that neogenin was expressed on 12.4±8.5% and 17.9±10.5% of $CD3^+$ cells in biopsies either with isolated (Fig 8A) or focal (Fig 8B) infiltrates respectively. We interpret these findings to suggest that the expression of neogenin on T cells is of great pathophysiological significance in vivo, and that it functions to elicit a T cell chemokinetic response in the process of T cell infiltration into human allografts.

Discussion

In this study, we show that the axonal guidance molecule Netrin-1 stimulates bi-directional migration of human $CD4^+$ T cells. Our results are based on the use of a novel microfluidic

device that allows for the characterization of migration in terms of directionality, speed and persistence at single cell resolution. Our findings indicate that Netrin-1 increases the fraction of migrating $CD4^+$ cells and stimulates bi-directional chemokinesis, but it does not alter the directionality or the speed of the motile cells *in vitro*. shRNA knockdown of neogenin in human $CD4^+$ T cells has marked effects to inhibit bi-directional migration and chemokinesis suggesting that Netrin-1/neogenin interactions elicit these migratory responses. When administered *in vivo*, Netrin-1 increases the local accumulation of neogenin-expressing $CD3^+$ T cell infiltrates into human skin on the huSCID mouse. In addition, neogenin co-localizes with CD3 on infiltrates within human endomycardial biopsies from cardiac transplant recipients. Collectively, these findings suggest that Netrin-1/neogenin interactions are pathophysiological to enhance T cell chemokinesis in association with acute inflammation and allograft rejection.

The biology of Netrin-1 is complex due to its potential to interact with both chemoattractive and chemorepulsive receptors on activated $CD4^+$ T cells. Indeed, the reported effects of Netrin-1 in inflammation are controversial. Netrin-1 has been previously described as an anti-inflammatory guidance protein via its binding to chemorepellent UNC5B in the absence of neogenin (4, 15). This effect was reported to be mediated in part via its effects on the local infiltration of neutrophils and macrophages (16, 18, 20, 34). However, more recent studies indicate that the expression of pro-migratory neogenin may be critical in the functional outcome of an inflammatory response (25–27, 35, 36). For example, inflammation is reduced in neogenin knockout mice in models of peritonitis, lung injury and ischemia-reperfusion. Thus, contrary to its reported anti-inflammatory effects, these findings support the interpretation that Netrin-1 has pro-inflammatory properties via interactions with distinct neogenin-expressing leukocyte subsets (25–27). Our new findings in this report indicate that the key function of Netrin-1 on CD4+ T lymphocytes is to induce chemokinesis, and that its effect on either chemoattraction or chemorepulsion are a function of random directional migration and/or additional factors.

Unlike traditional assays that define migration in a single direction, these studies have characterized migration using four quantitative parameters that include the fraction of cells responding, directionality, speed, and directional persistence. In this manner, we believe our results illustrate new concepts and paradigms about the biology of Netrin-1 and its associated induction of migratory responses in human T cells. For instance, while previous studies have identified either chemoattractant or chemorepellent properties of Netrin-1, our studies demonstrate that its biological effects on $CD4^+$ T-cells are multiparameter, resulting in a chemokinetic migratory response similar to C5a- and IL-8 (12). Furthermore, contrary to previous reports showing that Netrin-1/UNC5A/B interactions dominate and induce chemorepulsion, we did not observe repellant migratory patterns in neogenin knockdown cells. Rather, we observed a significant decrease of the population of migrating cells, without changes in directionality, similar to the effects of Slit2 on neutrophils (12). These new findings suggest that neuronal repellant cues inhibit leukocyte migratory activity, rather than inducing a true repellant migratory response.

Our *in vitro* studies indicate that Netrin-1/neogenin interactions provide a stimulus for $CD4^+$ T cell migration either towards or away from a gradient, and that directionality is dependent

on the presence of additional chemoattractive or repulsive cues. However, the addition of Netrin-1 did not alter the potent chemoattractant effects of the chemokine RANTES (37–39). Thus, while RANTES elicits a maximal signaling response resulting in chemoattraction, it is possible that Netrin-1/repellant receptor interactions only inhibit select signaling pathways. Overall, we interpret these data to indicate that Netrin-1/Netrin-1 receptor interactions on T cells may be independent or dependent on other cues and that the expression of neogenin is of major biological significance in the migratory response.

Several Netrin-1 regulated signaling pathways have potential to mediate these observed migratory responses. For example, Rho GTPases, including Rho, Rac and Cdc42, are key elements in the control of cell shape, actin cytoskeleton reorganization, and cell motility (40). Netrin-1 activates RhoA in glioblastoma and endothelial cells, enhancing the integrity of F-actin cytoskeleton, thereby inducing cell migration and invasion (41). Rac1 and Cdc42 are also required for Netrin-1-induced axon outgrowth and neuronal cell migration during development (42, 43). Collectively, these findings are most suggestive that Netrin-1 augments Rho GTPases which in turn elicit key migratory signals in T cells (44). Finally, Netrin-1 activates both focal adhesion kinase (FAK) and Src kinase (45, 46), which may also function as key signals for chemotaxis (47). Thus there are several Netrin-1 induced signaling responses to explain our observations and the diverse promigratory effects of T cell neogenin.

Our observations also suggest that there is some redundancy in the function of chemorepulsive UNC5 receptors on $CD4^+$ T cells. Consistent with this interpretation, medulloblastoma cells that express both neogenin and UNC5B respond to Netrin-1 with a marked migratory response resulting in increased invasiveness and angiogenesis (23). Thus, when multiple receptors are expressed by an individual cell type, high affinity binding to neogenin may allow for a dominant activation response. In contrast, in the absence of neogenin, the binding of Netrin-1 to UNC5 family receptor(s) alone can result in chemoinhibition. Interestingly, UNC5A/B may also serve as a co-receptor for neogenin, as has been described for *Repulsive Guidance Molecule-A* (RGMa) (48). Collectively, these reports allow for the interpretation that Netrin-1/UNC5A/B interactions may be anti-inflammatory, but that these effects are redundant once Netrin-1 binds neogenin.

Finally, to translate our in vitro findings in vivo, we used an established huSCID mouse model in which it is possible to administer Netrin-1 at the local inflammatory site and test its effects on the recruitment of human lymphocytes in vivo. Based on our in vitro data, we anticipated that Netrin-1 has potential to be both pro-inflammatory and/or pro-resolution in vivo depending on the local microenvironment. However, we observed that local Netrin-1 augments lymphocyte recruitment diffusely throughout the inflammatory site, which is consistent with its observed effect of chemokinesis. Furthermore, we found abundant neogenin expression on both infiltrating lymphocytes and on other cell types, including endothelial cells. Previous work has already established that neogenin is expressed by endothelial cells, and that Netrin-1 may function as an angiogenic factor (23, 49). This allows for the interpretation that the local overexpression of Netrin-1 promotes inflammation via its direct interactions with infiltrating $CD4^+$ T-cells and perhaps via indirect effects on endothelial activation. Furthermore, the pathophysiological importance of neogenin in T cell

recruitment is supported by our finding that it is expressed on CD3+ T-cells in rejecting human cardiac allografts. However, we have not excluded the possibility that these interactions may also promote chemokinesis for the emigration of lymphocytes out of tissues in the resolution phase of inflammation. Collectively, the novelty of these findings are that Netrin-1/neogenin interactions elicit bi-directional chemokinetic migration in $CD4^+$ T effectors but not in T regulatory cell subpopulations. Neogenin is expressed on activated lymphocytes in vivo in human allografts, and Netrin-1 promotes inflammation in human skin in the huSCID mouse. The translational implications of these findings is that targeting neogenin will likely have potent effects to inhibit cell-mediated immune responses, acute and chronic inflammation and lymphocyte recruitment into allografts.

Supplementary Material

Refer to Web version on PubMed Central for supplementary material.

Acknowledgments

We thank Sarah Bruneau PhD, Nora Kochupurakkal PhD, Kaifeng Liu MD PhD and Elisabeth Wong BS for support with techniques and interpretation of the results of these studies. We also thank Evelyn Flynn and Josephine Koch BS for general help with cellular staining and immunohistochemistry, and Janine van Gils PhD and Diane Bielenberg PhD for useful discussions. Finally, we wish to thank Tomoshige Akino MD for help with qPCR analysis.

References

1. Tessier-Lavigne M, Goodman CS. The molecular biology of axon guidance. Science. 1996; 274:1123–1133. [PubMed: 8895455]
2. Klagsbrun M, Eichmann A. A role for axon guidance receptors and ligands in blood vessel development and tumor angiogenesis. Cytokine & growth factor reviews. 2005; 16:535–548. [PubMed: 15979925]
3. Gaur P, Bielenberg DR, Samuel S, Bose D, Zhou Y, Gray MJ, Dallas NA, Fan F, Xia L, Lu J, Ellis LM. Role of class 3 semaphorins and their receptors in tumor growth and angiogenesis. Clinical cancer research: an official journal of the American Association for Cancer Research. 2009; 15:6763–6770. [PubMed: 19887479]
4. Ly NP, Komatsuzaki K, Fraser IP, Tseng AA, Prodhan P, Moore KJ, Kinane TB. Netrin-1 inhibits leukocyte migration in vitro and in vivo. Proceedings of the National Academy of Sciences of the United States of America. 2005; 102:14729–14734. [PubMed: 16203981]
5. van Gils JM, Derby MC, Fernandes LR, Ramkhelawon B, Ray TD, Rayner KJ, Parathath S, Distel E, Feig JL, Alvarez-Leite JI, Rayner AJ, McDonald TO, O'Brien KD, Stuart LM, Fisher EA, Lacy-Hulbert A, Moore KJ. The neuroimmune guidance cue netrin-1 promotes atherosclerosis by inhibiting the emigration of macrophages from plaques. Nat Immunol. 13:136–143. [PubMed: 22231519]
6. Wu JY, Feng L, Park HT, Havlioglu N, Wen L, Tang H, Bacon KB, Jiang Z, Zhang X, Rao Y. The neuronal repellent Slit inhibits leukocyte chemotaxis induced by chemotactic factors. Nature. 2001; 410:948–952. [PubMed: 11309622]
7. Takamatsu H, Kumanogoh A. Diverse roles for semaphorin-plexin signaling in the immune system. Trends Immunol. 2012; 33:127–135. [PubMed: 22325954]
8. Battaglia A, Buzzonetti A, Monego G, Peri L, Ferrandina G, Fanfani F, Scambia G, Fattorossi A. Neuropilin-1 expression identifies a subset of regulatory T cells in human lymph nodes that is modulated by preoperative chemoradiation therapy in cervical cancer. Immunology. 2008; 123:129–138. [PubMed: 18028372]

9. Solomon BD, Mueller C, Chae WJ, Alabanza LM, Bynoe MS. Neuropilin-1 attenuates autoreactivity in experimental autoimmune encephalomyelitis. Proceedings of the National Academy of Sciences of the United States of America. 2011; 108:2040–2045. [PubMed: 21245328]
10. Kumanogoh A, Kikutani H. Immunological functions of the neuropilins and plexins as receptors for semaphorins. Nature reviews Immunology. 2013; 13:802–814.
11. Chaturvedi S, Yuen DA, Bajwa A, Huang YW, Sokollik C, Huang L, Lam GY, Tole S, Liu GY, Pan J, Chan L, Sokolskyy Y, Puthia M, Godaly G, John R, Wang C, Lee WL, Brumell JH, Okusa MD, Robinson LA. Slit2 prevents neutrophil recruitment and renal ischemia-reperfusion injury. J Am Soc Nephrol. 2013; 24:1274–1287. [PubMed: 23766538]
12. Boneschansker L, Yan J, Wong E, Briscoe DM, Irimia D. Microfluidic platform for the quantitative analysis of leukocyte migration signatures. Nat Commun. 2014; 5:4787. [PubMed: 25183261]
13. Coulthard MG, Morgan M, Woodruff TM, Arumugam TV, Taylor SM, Carpenter TC, Lackmann M, Boyd AW. Eph/Ephrin signaling in injury and inflammation. Am J Pathol. 2012; 181:1493–1503. [PubMed: 23021982]
14. Kitamura T, Kabuyama Y, Kamataki A, Homma MK, Kobayashi H, Aota S, Kikuchi S, Homma Y. Enhancement of lymphocyte migration and cytokine production by ephrinB1 system in rheumatoid arthritis. Am J Physiol Cell Physiol. 2008; 294:C189–196. [PubMed: 17942634]
15. Tadagavadi RK, Wang W, Ramesh G. Netrin-1 regulates Th1/Th2/Th17 cytokine production and inflammation through UNC5B receptor and protects kidney against ischemia-reperfusion injury. J Immunol. 2010; 185:3750–3758. [PubMed: 20693423]
16. Ranganathan PV, Jayakumar C, Mohamed R, Dong Z, Ramesh G. Netrin-1 regulates the inflammatory response of neutrophils and macrophages, and suppresses ischemic acute kidney injury by inhibiting COX-2-mediated PGE2 production. Kidney Int. 2013; 83:1087–1098. [PubMed: 23447066]
17. Mehlen P, Delloye-Bourgeois C, Chedotal A. Novel roles for Slits and netrins: axon guidance cues as anticancer targets? Nature reviews Cancer. 2011; 11:188–197. [PubMed: 21326323]
18. Mirakaj V, Gatidou D, Potzsch C, Konig K, Rosenberger P. Netrin-1 signaling dampens inflammatory peritonitis. J Immunol. 2011; 186:549–555. [PubMed: 21098235]
19. Lai Wing Sun K, Correia JP, Kennedy TE. Netrins: versatile extracellular cues with diverse functions. Development. 2011; 138:2153–2169. [PubMed: 21558366]
20. Mirakaj V, Thix CA, Laucher S, Mielke C, Morote-Garcia JC, Schmit MA, Henes J, Unertl KE, Kohler D, Rosenberger P. Netrin-1 dampens pulmonary inflammation during acute lung injury. Am J Respir Crit Care Med. 2010; 181:815–824. [PubMed: 20075388]
21. Rosenberger P, Schwab JM, Mirakaj V, Masekowsky E, Mager A, Morote-Garcia JC, Unertl K, Eltzschig HK. Hypoxia-inducible factor-dependent induction of netrin-1 dampens inflammation caused by hypoxia. Nat Immunol. 2009; 10:195–202. [PubMed: 19122655]
22. Aherne CM, Collins CB, Masterson JC, Tizzano M, Boyle TA, Westrich JA, Parnes JA, Furuta GT, Rivera-Nieves J, Eltzschig HK. Neuronal guidance molecule netrin-1 attenuates inflammatory cell trafficking during acute experimental colitis. Gut. 2012; 61:695–705. [PubMed: 21813473]
23. Akino T, Han X, Nakayama H, McNeish B, Zurakowski D, Mammoto A, Klagsbrun M, Smith E. Netrin-1 promotes medulloblastoma cell invasiveness and angiogenesis, and demonstrates elevated expression in tumor tissue and urine of patients with pediatric medulloblastoma. Cancer research. 2014; 74:3716–3726. [PubMed: 24812271]
24. Ramkhelawon B, Hennessy EJ, Menager M, Ray TD, Sheedy FJ, Hutchison S, Wanschel A, Oldebeken S, Geoffrion M, Spiro W, Miller G, McPherson R, Rayner KJ, Moore KJ. Netrin-1 promotes adipose tissue macrophage retention and insulin resistance in obesity. Nature medicine. 20:377–384.
25. Konig K, Gatidou D, Granja T, Meier J, Rosenberger P, Mirakaj V. The axonal guidance receptor neogenin promotes acute inflammation. PloS one. 2012; 7:e32145. [PubMed: 22412855]
26. Mirakaj V, Jennewein C, Konig K, Granja T, Rosenberger P. The guidance receptor neogenin promotes pulmonary inflammation during lung injury. FASEB journal: official publication of the Federation of American Societies for Experimental Biology. 2012; 26:1549–1558. [PubMed: 22198383]

27. Schlegel M, Granja T, Kaiser S, Korner A, Henes J, Konig K, Straub A, Rosenberger P, Mirakaj V. Inhibition of neogenin dampens hepatic ischemia-reperfusion injury. Crit Care Med. 2014; 42:e610–619. [PubMed: 25029243]
28. Bielenberg DR, Shimizu A, Klagsbrun M. Semaphorin-induced cytoskeletal collapse and repulsion of endothelial cells. Methods Enzymol. 2008; 443:299–314. [PubMed: 18772022]
29. Jain NG, Wong EA, Aranyosi AJ, Boneschansker L, Markmann JF, Briscoe DM, Irimia D. Microfluidic mazes to characterize T-cell exploration patterns following activation in vitro. Integr Biol (Camb). 2015
30. Moulton KS, Melder RJ, Dharnidharka VR, Hardin-Young J, Jain RK, Briscoe DM. Angiogenesis in the huPBL-SCID model of human transplant rejection. Transplantation. 1999; 67:1626–1631. [PubMed: 10401773]
31. Melter M, Reinders ME, Sho M, Pal S, Geehan C, Denton MD, Mukhopadhyay D, Briscoe DM. Ligation of CD40 induces the expression of vascular endothelial growth factor by endothelial cells and monocytes and promotes angiogenesis in vivo. Blood. 2000; 96:3801–3808. [PubMed: 11090063]
32. Reinders ME, Sho M, Izawa A, Wang P, Mukhopadhyay D, Koss KE, Geehan CS, Luster AD, Sayegh MH, Briscoe DM. Proinflammatory functions of vascular endothelial growth factor in alloimmunity. J Clin Invest. 2003; 112:1655–1665. [PubMed: 14660742]
33. Edelbauer M, Datta D, Vos IH, Basu A, Stack MP, Reinders ME, Sho M, Calzadilla K, Ganz P, Briscoe DM. Effect of vascular endothelial growth factor and its receptor KDR on the transendothelial migration and local trafficking of human T cells in vitro and in vivo. Blood. 2010; 116:1980–1989. [PubMed: 20538805]
34. Chen J, Cai QP, Shen PJ, Yan RL, Wang CM, Yang DJ, Fu HB, Chen XY. Netrin-1 protects against L-Arginine-induced acute pancreatitis in mice. PloS one. 2012; 7:e46201. [PubMed: 23029434]
35. Mirakaj V, Brown S, Laucher S, Steinl C, Klein G, Kohler D, Skutella T, Meisel C, Brommer B, Rosenberger P, Schwab JM. Repulsive guidance molecule-A (RGM-A) inhibits leukocyte migration and mitigates inflammation. Proceedings of the National Academy of Sciences of the United States of America. 2011; 108:6555–6560. [PubMed: 21467223]
36. Muramatsu R, Kubo T, Mori M, Nakamura Y, Fujita Y, Akutsu T, Okuno T, Taniguchi J, Kumanogoh A, Yoshida M, Mochizuki H, Kuwabara S, Yamashita T. RGMa modulates T cell responses and is involved in autoimmune encephalomyelitis. Nature medicine. 2011; 17:488–494.
37. el-Sawy T, Fahmy NM, Fairchild RL. Chemokines: directing leukocyte infiltration into allografts. Curr Opin Immunol. 2002; 14:562–568. [PubMed: 12183154]
38. Panzer U, Reinking RR, Steinmetz OM, Zahner G, Sudbeck U, Fehr S, Pfalzer B, Schneider A, Thaiss F, Mack M, Conrad S, Huland H, Helmchen U, Stahl RA. CXCR3 and CCR5 positive T-cell recruitment in acute human renal allograft rejection. Transplantation. 2004; 78:1341–1350. [PubMed: 15548973]
39. Baggiolini M. Chemokines and leukocyte traffic. Nature. 1998; 392:565–568. [PubMed: 9560152]
40. Ridley AJ. Rho GTPase signalling in cell migration. Curr Opin Cell Biol. 2015; 36:103–112. [PubMed: 26363959]
41. Shimizu A, Nakayama H, Wang P, Konig C, Akino T, Sandlund J, Coma S, Italiano JE Jr, Mammoto A, Bielenberg DR, Klagsbrun M. Netrin-1 promotes glioblastoma cell invasiveness and angiogenesis by multiple pathways including activation of RhoA, cathepsin B, and cAMP-response element-binding protein. J Biol Chem. 2013; 288:2210–2222. [PubMed: 23195957]
42. Briancon-Marjollet A, Ghogha A, Nawabi H, Triki I, Auziol C, Fromont S, Piche C, Enslen H, Chebli K, Cloutier JF, Castellani V, Debant A, Lamarche-Vane N. Trio mediates netrin-1-induced Rac1 activation in axon outgrowth and guidance. Mol Cell Biol. 2008; 28:2314–2323. [PubMed: 18212043]
43. Causeret F, Hidalgo-Sanchez M, Fort P, Backer S, Popoff MR, Gauthier-Rouviere C, Bloch-Gallego E. Distinct roles of Rac1/Cdc42 and Rho/Rock for axon outgrowth and nucleokinesis of precerebellar neurons toward netrin 1. Development. 2004; 131:2841–2852. [PubMed: 15151987]
44. Rougerie P, Delon J. Rho GTPases: masters of T lymphocyte migration and activation. Immunol Lett. 2012; 142:1–13. [PubMed: 22207038]

45. Ren XR, Ming GL, Xie Y, Hong Y, Sun DM, Zhao ZQ, Feng Z, Wang Q, Shim S, Chen ZF, Song HJ, Mei L, Xiong WC. Focal adhesion kinase in netrin-1 signaling. Nat Neurosci. 2004; 7:1204–1212. [PubMed: 15494733]

46. Li W, Lee J, Vikis HG, Lee SH, Liu G, Aurandt J, Shen TL, Fearon ER, Guan JL, Han M, Rao Y, Hong K, Guan KL. Activation of FAK and Src are receptor-proximal events required for netrin signaling. Nat Neurosci. 2004; 7:1213–1221. [PubMed: 15494734]

47. Korade-Mirnics Z, Corey SJ. Src kinase-mediated signaling in leukocytes. J Leukoc Biol. 2000; 68:603–613. [PubMed: 11073097]

48. Hata K, Kaibuchi K, Inagaki S, Yamashita T. Unc5B associates with LARG to mediate the action of repulsive guidance molecule. J Cell Biol. 2009; 184:737–750. [PubMed: 19273616]

49. Park KW, Crouse D, Lee M, Karnik SK, Sorensen LK, Murphy KJ, Kuo CJ, Li DY. The axonal attractant Netrin-1 is an angiogenic factor. Proceedings of the National Academy of Sciences of the United States of America. 2004; 101:16210–16215. [PubMed: 15520390]

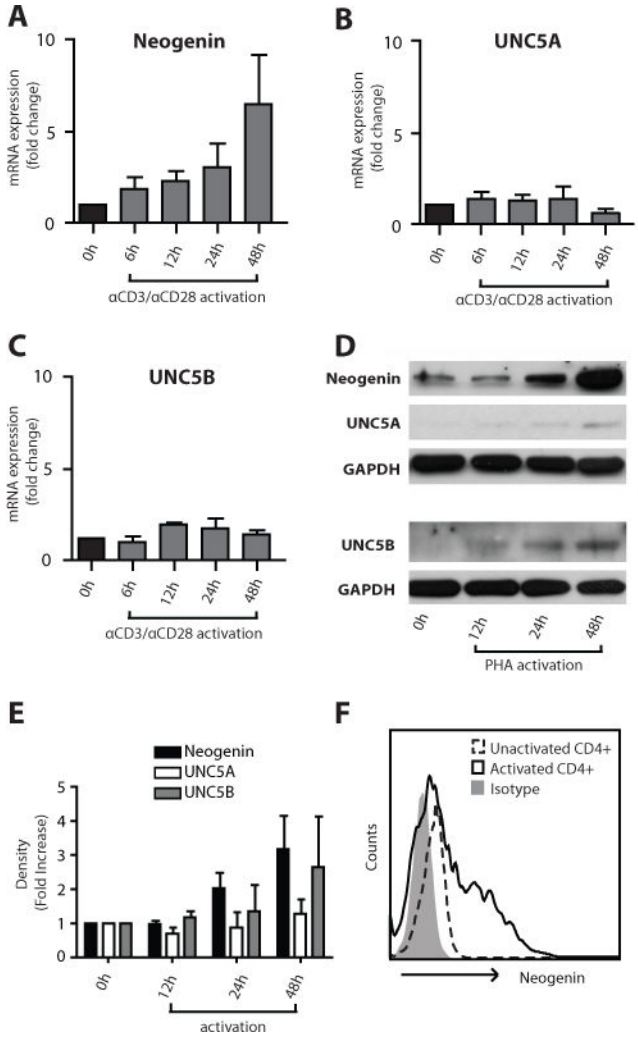

Figure 1. Netrin-1 receptor expression by human CD4$^+$ T lymphocytes

The expression of known Netrin-1 receptors was analyzed at the mRNA level by quantitative PCR (Panels A–C), at the protein level by Western blot analysis (Panels D–E) and by FACS after 48hrs activation (Panel F). Panels A–C show the mean fold change in mRNA expression ±SEM. In Panel D, induced expression of neogenin, UNC5A and UNC5B is illustrated and Panel E illustrates densitometric analysis of n=3 independent Western blots. The illustrated data in Panels A-F are representative of n=3 independent experiments.

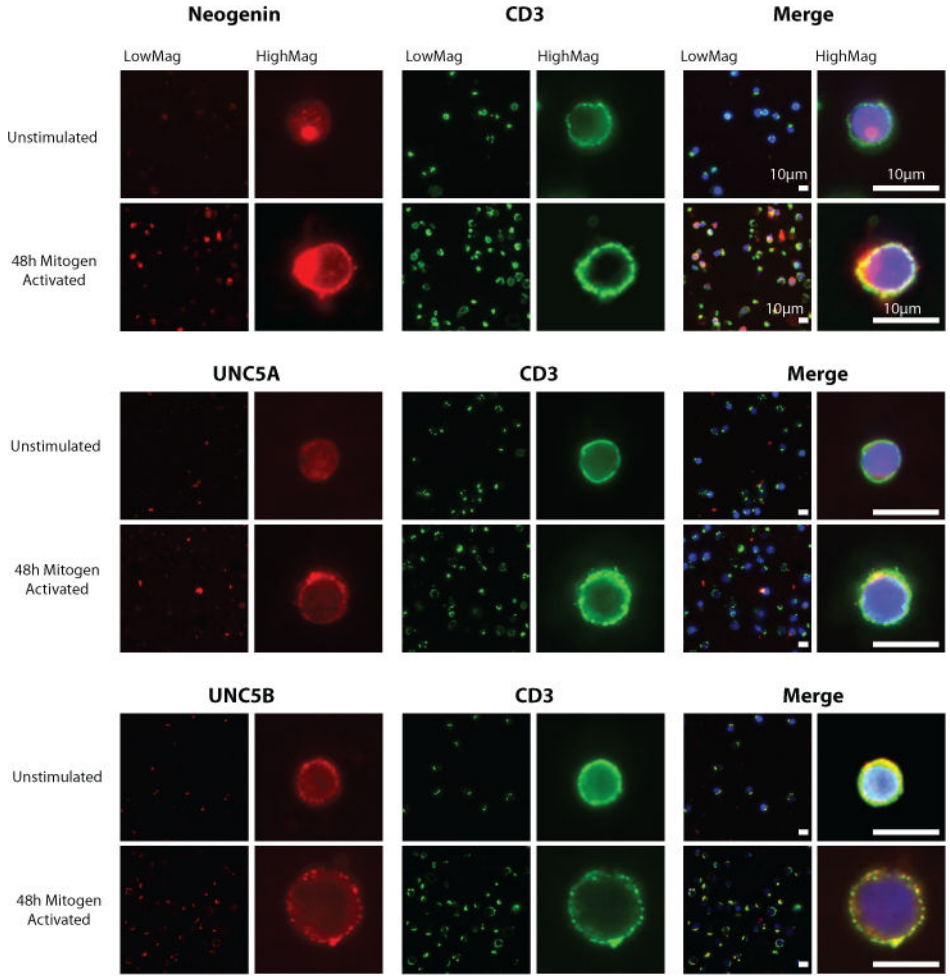

Figure 2. Localization of Neogenin, UNC5A and UNC5B on CD4$^+$ T cells

Expression of the Netrin-1 receptors Neogenin, UNC5A and UNC5B was analyzed on unactivated or mitogen-dependent activated (PHA 2.5μg/mL) human CD4$^+$ T cells by immunofluorescent staining. Netrin-1 receptor expression (red) is illustrated on cells stained with anti-CD3 (green) and colocalization is seen in the merged image as a yellow stain. All images are representative of n=3 independent experiments.

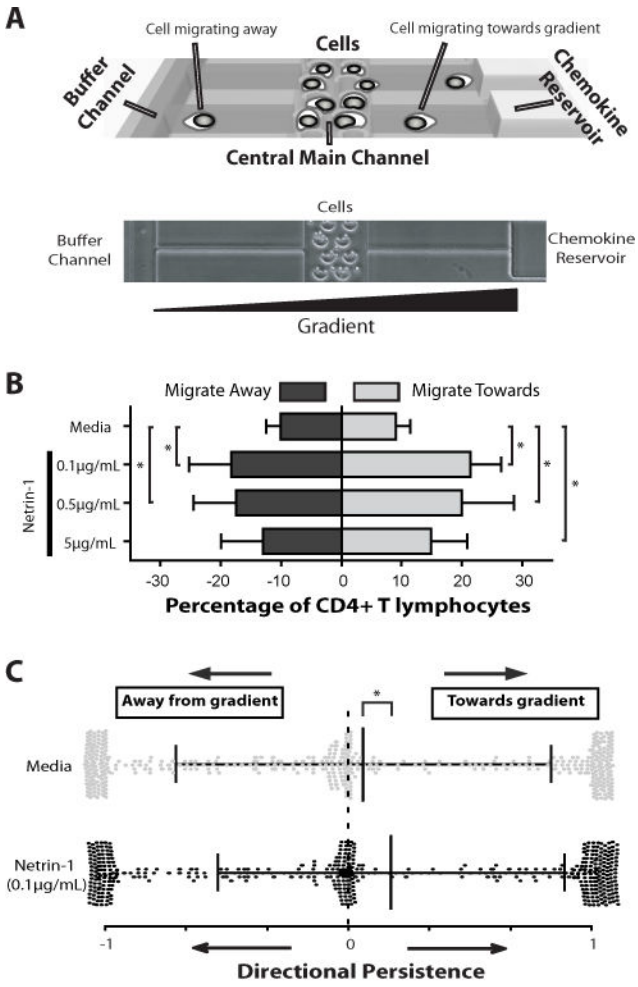

Figure 3. Netrin-1 increases both the size, and the chemokinetic response of migrating CD4$^+$ T cells

CD4$^+$ T cell migration was analyzed in a microfluidic device that allows for the quantitative analysis of the fraction of migrating cells, their directionality, persistence and speed at the single cell level. Panel A illustrates the microfluidic device. CD4$^+$ T cells are loaded into the central main channel and are monitored in real-time migrating through 10-micron side channels over an 8hr time period. Each cell has potential to migrate either towards (direction of reservoir) or away (direction of buffer channel) from a chemokine gradient. Panel B illustrates the quantitative analysis of bi-directional migratory patterns of 48h mitogen-activated CD4$^+$ T cells (αCD3/αCD28 1µg/mL each) in response to increasing concentrations of Netrin-1, as indicated. Grey bars represent migration towards the gradient, and black bars represent migration away from the gradient (mean±SD of n=≥3 independent experiments). Panel C shows a scatter plot of migratory directional persistence of CD4$^+$ cells in response to Netrin-1. The migratory patterns of individual CD4$^+$ T cells were evaluated and are illustrated as either grey dots (media alone) or black dots (response to Netrin-1). The black lines represent the median and standard deviation of migratory responses under each condition. Number of cells analyzed in media alone was 449/2232 total migrating cells, and

in Netrin-1 was 399/1068 total migrating cells. Illustrated data is from n=3 independent experiments. * =p< 0.05.

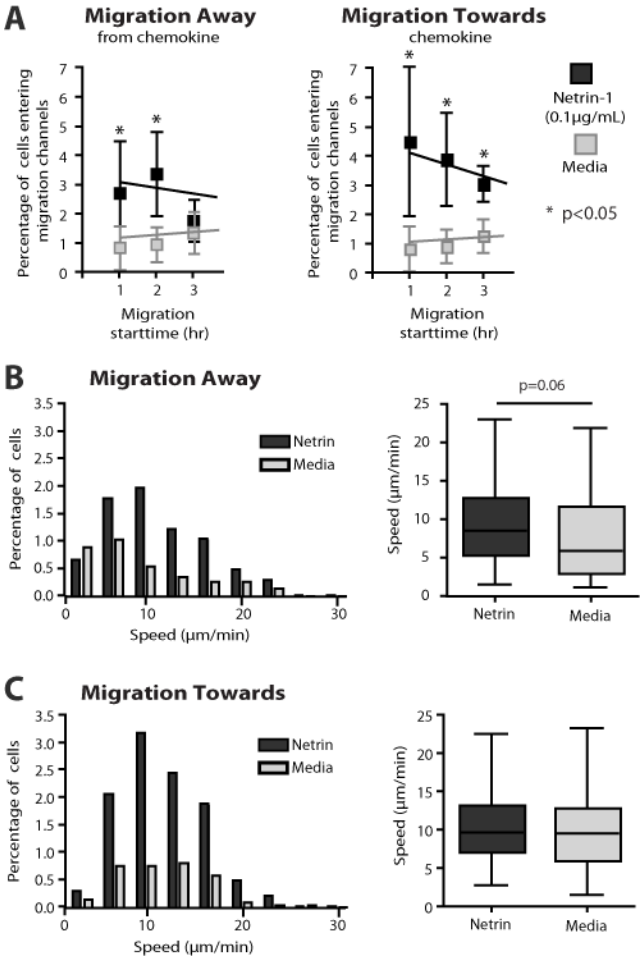

Figure 4. Migration characteristics of CD4$^+$ T lymphocytes in response to Netrin-1

Migration patterns of individual T cells were analyzed using time-lapse videos over an 8hr time period. Panel A illustrates the time-distribution of the initial migratory response and the hourly response over the course of each experiment. The effect of Netrin-1 was prominent in the first 3 hours of migration. Black symbols represent cell migration in response to Netrin-1, whereas grey symbols represent response in media alone. In Panels B–C, the percentage of cells that migrate at each indicated speed (in µm/min) is separated into groups of 3.3 µm/min intervals, for cells migrating away from the gradient (B) and towards the gradient (C). Black bars represent cells migrating in response to Netrin-1, and grey bars represent cells migrating in response to media alone (as a control). The average migratory speed for each condition is shown in the box and whiskers plot. Error bars represent mean ±SD. The number of cells analyzed in media was 449/2232 total and in Netrin-1 was 399/1069 total. Illustrated data is from n≥3 independent experiments. * =p< 0.05.

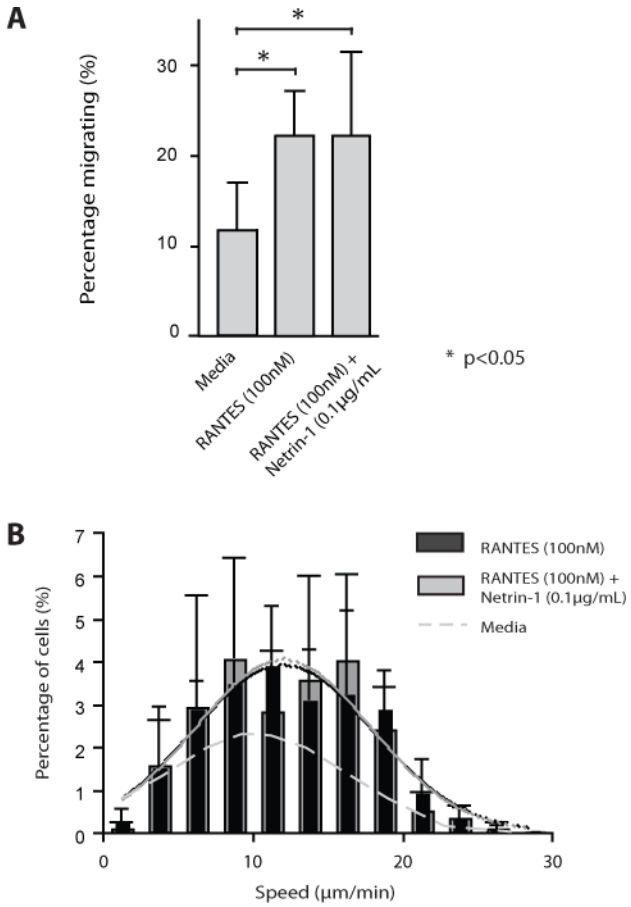

Figure 5. Effect of Netrin-1 on RANTES-induced migration

$CD4^+$ T cells were loaded in the microfluidic device, and were exposed to a RANTES gradient in the absence or presence of Netrin-1 (0.1µg/ml). Panel A represents the percentage of cells migrating in the direction of the gradient over an 8 hr time period. Panel B illustrates the migratory speed of individual T cells. The black bars represent migratory speed induced by RANTES, and the grey bars represent migration speed in response to both RANTES and Netrin-1. The dashed gray line illustrates the speed distribution in media alone. Solid grey and black lines illustrate the distribution of migratory speed for RANTES with (grey) or without (black) Netrin-1. Illustrated is the combined data from n=3 independent experiments showing responses in n=377 migrating cells (RANTES alone) and n=256 migrating cells (RANTES + Netrin-1). Bars represent the mean±SD. * =p< 0.05.

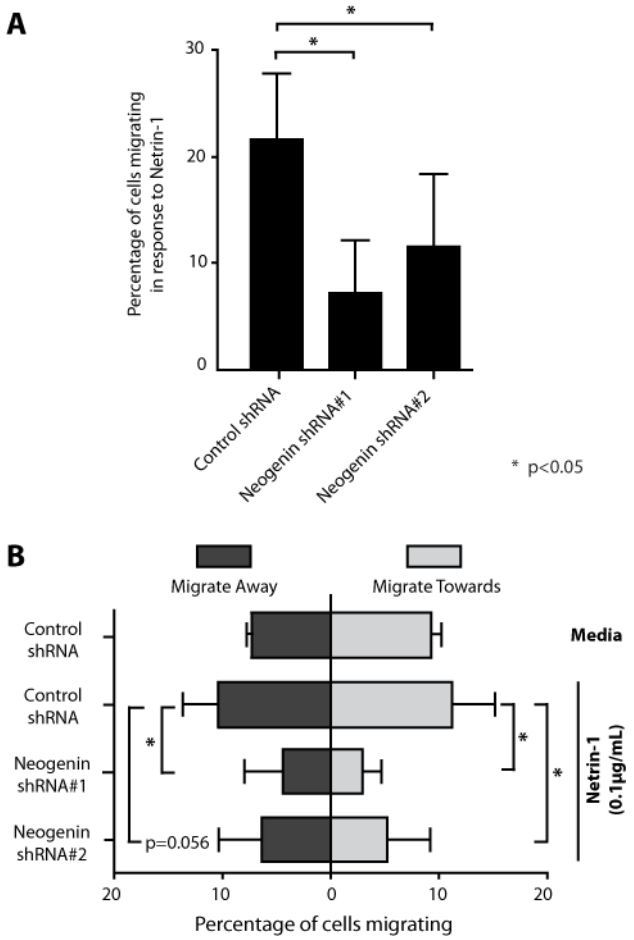

Figure 6. Knockdown of neogenin attenuates the migratory response to Netrin-1

Human $CD4^+$ T-cells were infected with two neogenin shRNAs, each yielding a knockdown efficiency of 50–70% (as shown in Figure S3). Control shRNA or neogenin shRNA-infected $CD4^+$ T cells were loaded into microfluidic devices and the percentage of cells migrating in response to Netrin-1 was evaluated (Panel A). In Panel B, bi-directional migratory patterns were evaluated in response to Netrin-1 (0.1 μg/ml) vs. media alone using control shRNA or neogenin shRNA-infected $CD4^+$ T cells. Error bars represent mean±SD. Data shown is from n=3 independent experiments with a total of n=1120 (Neogenin shRNA#1), n=1324 (Neogenin shRNA#2) and n= 1222 (Control shRNA) analyzed cells. * =p< 0.05.

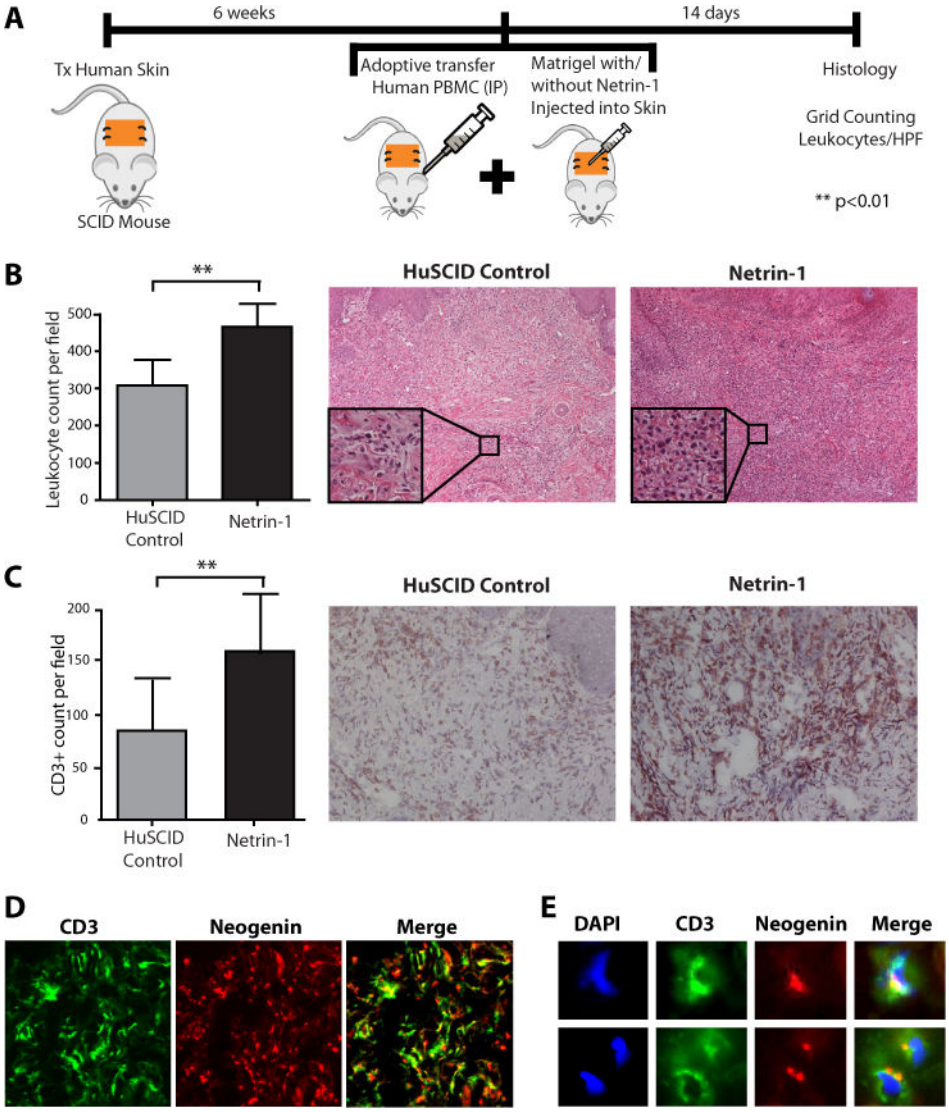

Figure 7. Effect of Netrin-1 on leukocyte infiltration in vivo

Panel A: Cartoon illustrating the huSCID model; human skin is transplanted onto SCID mice, and after 6 weeks the mice are humanized by i.p. injection of 3×10^8 human PBMC. On day 0 and day 7, Netrin-1/matrigel (5μg) or matrigel alone is injected subcutaneously into the human skin graft (n=8 mice). Panel B, H&E staining of human skin samples harvested on day 14 post humanization. Representative histology is shown in the right panels (100× mag; box insert 400× mag); the average number of infiltrates in each skin was grid counted (as described (30)) and is shown in the left bar graph (n=8 skins; **p<0.01). Panel C shows representative cryosections from day 14 skin samples immunostained with anti-CD3; the number of $CD3^+$ T cells was grid counted and the average $CD3^+$ T cell count (mean±SD) is illustrated in the bar graph (left panel) (n=8, **p<0.01). Panel D shows representative immunofluorescent staining of a Netrin-1-treated human skin graft using anti-neogenin (red stain) and anti-CD3 (green stain) and colocalization is seen in the merged image as yellow color. Panel E shows high magnification (400×) immunofluorescent images

of Panel D, showing polarized expression of Neogenin receptors on the T cell surface as the merged yellow image. Nuclei are stained with DAPI (blue).

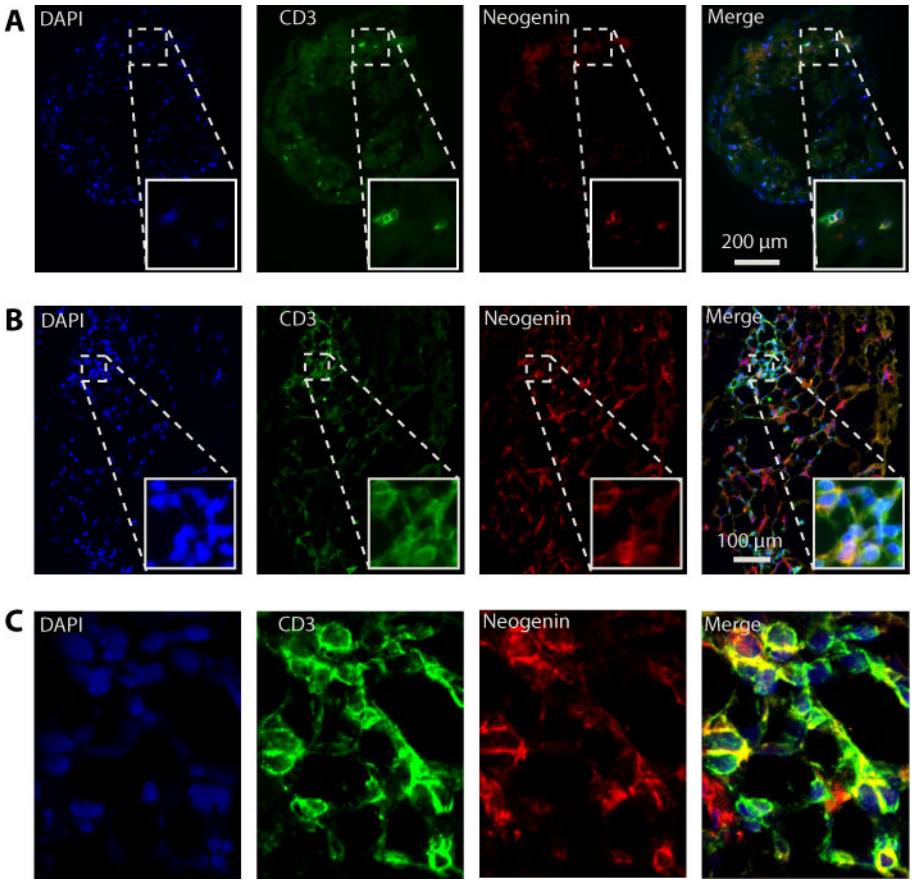

Figure 8. Expression of neogenin on lymphocytes within human cardiac allografts

Panel A: Immunofluorescence staining of CD3 and neogenin in a representative biopsy from a cardiac allograft with sparse CD3+ T cell infiltrates. Illustrated is coexpression of neogenin with CD3 on an isolated infiltrating lymphocyte (100× mag; box insert 200× mag). Panel B: High power photomicrograph of a representative biopsy showing colocalization of neogenin with CD3 within a focal infiltrate (200× mag; box insert 400× mag). Panel C: Confocal microscopy illustrating coexpression of CD3 and neogenin on a focal infiltrate within an allograft biopsy.